

Differential Mapping of Depolarization Component of Mueller Matrix of Optically Thick Biological Layers

Yu. Solovey¹⁾, O.Ushenko²⁾, V.Zhytaryuk²⁾, O. Dubolazov²⁾, V. Ushenko²⁾,
M. Kovalchuk²⁾, O. Yatsko²⁾

¹⁾ Bukovinian State Medical University, 3 Theatral Sq., Chernivtsi, Ukraine, 58000

²⁾ Chernivtsi National University, 2 Kotsiubynskyi Str., Chernivtsi, Ukraine, 58012

ABSTRACT

This report contains theoretical algorithm for the differential representation of a phase-inhomogeneous biological object as a set of consecutively located optically anisotropic layers; theoretical algorithms for the decomposition of the Mueller-matrix of the diffuse biological layer in the basis of differential matrices of the 1st and 2nd orders; analytical relations for determining the magnitude of the set of elements of differential matrices of the 1st and 2nd orders; information and characteristics of optical schemes of experimental devices.

Keywords: Mueller matrix, biological layer, depolarizing component, diagnostic.

1. Introduction

The theoretical analysis of the distributions of the magnitude of the elements of depolarization of the component of the Mueller matrix is based on our generalized Azzam-Osikovskiy theory^{1,2} for the case of spectrally selective sounding of an optically thick biological layer and reproduction of the distribution of fluctuations of the optical anisotropy parameters, as well as its model addition, was proposed by V. Devlamink in³. Here, the magnitude of each of the elementary polarization properties $\xi_{i=1-6}$ of the scattering medium is considered as the average μ_i and fluctuating σ_i components

$$\xi_i = \mu_i + \sigma_i; \quad (1)$$

$$\bar{\xi}_i = \mu_i; \bar{\sigma}_i = 0. \quad (2)$$

Here

$$\mu_i = \begin{pmatrix} \mu_1 = LD \\ \mu_2 = CD \\ \mu_3 = LD' \\ \mu_4 = LB \\ \mu_5 = CB \\ \mu_6 = LB' \end{pmatrix}; \sigma_i = \begin{pmatrix} \sigma_1 = \sqrt{D_{LD}} \\ \sigma_2 = \sqrt{D_{CD}} \\ \sigma_3 = \sqrt{D_{LD'}} \\ \sigma_4 = \sqrt{D_{LB}} \\ \sigma_5 = \sqrt{D_{CB}} \\ \sigma_6 = \sqrt{D_{LB'}} \end{pmatrix}, \quad (3)$$

where $\sqrt{D_i}$ - standard deviation of fluctuations in polarization properties.

In approximation (1) - (3), V. Devlamink³ obtained the following expression for a second-order differential matrix

$$\{\Delta m^2\} = \begin{vmatrix} (\bar{\sigma}_4^2 + \bar{\sigma}_5^2 + \bar{\sigma}_6^2)_{11} & -0,5(\bar{\sigma}_2\bar{\sigma}_6 - \bar{\sigma}_3\bar{\sigma}_5)_{12} & -0,5(\bar{\sigma}_3\bar{\sigma}_4 - \bar{\sigma}_1\bar{\sigma}_6)_{13} & -0,5(\bar{\sigma}_1\bar{\sigma}_5 - \bar{\sigma}_2\bar{\sigma}_4)_{14} \\ 0,5(\bar{\sigma}_2\bar{\sigma}_6 - \bar{\sigma}_3\bar{\sigma}_5)_{21} & (\bar{\sigma}_4^2 - \bar{\sigma}_2^2 - \bar{\sigma}_3^2)_{22} & 0,5(\bar{\sigma}_1\bar{\sigma}_2 + \bar{\sigma}_4\bar{\sigma}_5)_{23} & 0,5(\bar{\sigma}_1\bar{\sigma}_3 + \bar{\sigma}_4\bar{\sigma}_5)_{24} \\ 0,5(\bar{\sigma}_3\bar{\sigma}_4 - \bar{\sigma}_1\bar{\sigma}_6)_{31} & 0,5(\bar{\sigma}_1\bar{\sigma}_2 + \bar{\sigma}_4\bar{\sigma}_5)_{32} & (\bar{\sigma}_5^2 - \bar{\sigma}_1^2 - \bar{\sigma}_3^2)_{33} & 0,5(\bar{\sigma}_2\bar{\sigma}_3 + \bar{\sigma}_5\bar{\sigma}_6)_{34} \\ 0,5(\bar{\sigma}_1\bar{\sigma}_5 - \bar{\sigma}_2\bar{\sigma}_4)_{41} & 0,5(\bar{\sigma}_1\bar{\sigma}_3 + \bar{\sigma}_4\bar{\sigma}_6)_{42} & 0,5(\bar{\sigma}_2\bar{\sigma}_3 + \bar{\sigma}_5\bar{\sigma}_6)_{43} & (\bar{\sigma}_6^2 - \bar{\sigma}_1^2 - \bar{\sigma}_3^2)_{44} \end{vmatrix} \quad (4)$$

An analysis of expression (4) reveals the following physical meaning of the partial elements of the depolarization component of the Mueller matrix of an optical-thick biological layer with fluctuations in the parameters of linear and circular birefringence and dichroism:

- diagonal elements $\{\Delta m^2\}_{ii}$ of a second-order differential matrix are determined by combinations of the magnitude of dispersion D_i of fluctuations in the parameters of various mechanisms of phase and amplitude anisotropy of an optically thick layer of biological tissue;
- diagonal elements $\{\Delta m^2\}_{i \neq k}$ represent the degree of correlation between fluctuations of various polarization properties of linear and circular birefringence and the dichroism of the polycrystalline component of biological layers.

It should be noted that with an increase in the light scattering frequency in the volume of the biological layer, the degree of correlation between the parameters of various mechanisms of phase and amplitude anisotropy decreases and tends to zero. Due to this, the second-order differential matrix operator (the depolarization component of the Mueller matrix) takes the form

$$\{\Delta m^2\} = \begin{vmatrix} (\bar{\sigma}_4^2 + \bar{\sigma}_5^2 + \bar{\sigma}_6^2)_{11} & 0 & 0 & 0 \\ 0 & (\bar{\sigma}_4^2 - \bar{\sigma}_2^2 - \bar{\sigma}_3^2)_{22} & 0 & 0 \\ 0 & 0 & (\bar{\sigma}_5^2 - \bar{\sigma}_1^2 - \bar{\sigma}_3^2)_{33} & 0 \\ 0 & 0 & 0 & (\bar{\sigma}_6^2 - \bar{\sigma}_1^2 - \bar{\sigma}_3^2)_{44} \end{vmatrix} \quad (5)$$

Thus, off-diagonal elements $\{\Delta m^2\}_{ii}$ are treatment-sensitive to changes in the polycrystalline structure of biological layers under transitional conditions from partial to severe depolarization. The boundary depolarization conditions are studies of diagonal matrix elements $\{\Delta m^2\}_{i \neq k}$, the magnitude of which is correlated with the dispersion $\bar{\sigma}_i^2$ of fluctuations of linear and circular birefringence and dichroism of an optically thick biological layer with multiple light scattering.

2. Methods of experimental measurements

The measurements of coordinate distributions of Mueller-matrix elements were performed in the setup (Fig. 1) ⁴⁻⁸.

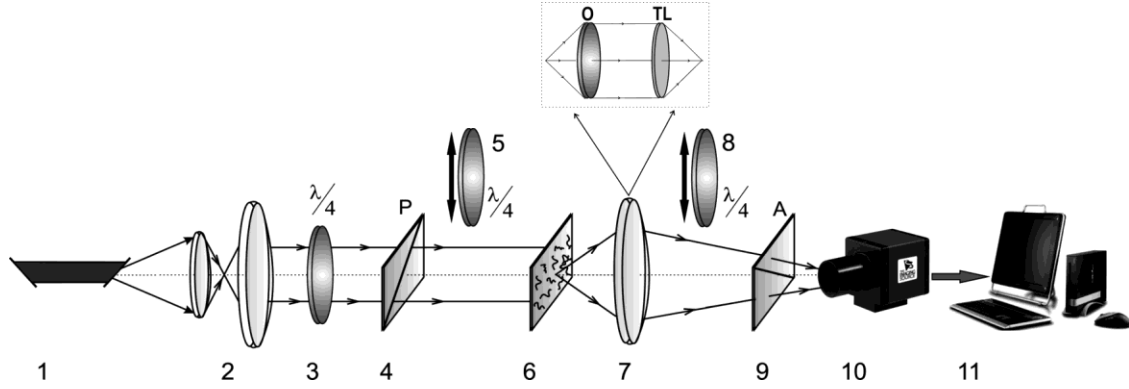


Fig. 1. Optical scheme of experimental setup. Here 1 – He-Ne laser; 2 – collimator; 3 – stationary quarter-wave plate; 5, 8 – mechanically movable quarter-wave plates; 4, 9 – polarizer and analyzer respectively; 6 – object of investigation; 7 – optical system; 10 – CCD camera; 11 – PC. Explanations are in the text.

Illumination of samples was performed by parallel ($\varnothing = 2 \times 10^3 \mu\text{m}$) weakly intensive ($W=5 \text{ mW}$) beam 1 of He-Ne laser ($\lambda = 0.6328 \mu\text{m}$). Using a collimated illuminating beam provides the same conditions of transformation of the polarization states at different points of the illuminated area of the object. In this case, our scheme provides the resolution of $4.65 \mu\text{m} \times 4.65 \mu\text{m}$. This scale is sufficient to evaluate the optical properties of the average ($5 \mu\text{m} - 20 \mu\text{m}$) crystalline structural elements of the of bile films. This allows comparative studies to differentiate different groups of samples. Polarization light source consisted of quarterwave plate 3 and polarizer 4. The image of samples 6 were projected in the plane of light-sensitive plane of CCD-camera 10 (The Imaging Source DMK 41AU02.AS, monochrome 1/2" CCD, Sony ICX205AL (progressive scan); resolution – 1280x960; size of light-sensitive plate – $5952 \mu\text{m} \times 4464 \mu\text{m}$; sensitivity – 0.05 lx; dynamic range – 8 bit; SNR – 9 bit, nonlinearity does not exceed 3%-5%) by means of optical system 7. In this experimental arrangement 7 designates an image forming apparatus, which consists of strain-free objective (Nikon CFI Achromat P, working distance – 30mm, focal distance - 50mm, NA – 0.1, magnification – 4x) and tube lens (focal distance 200mm). Polarization analysis of the samples images was performed by means of quarterwave plate 8 and polarizer-analyzer 9.

The calculation within each pixel of the digital camera 10 of the set of elements of the Mueller matrix of the sample of the biological layer was performed in accordance with the algorithm⁹⁻¹⁶

$$\begin{aligned}
 M_{11} &= 0.5(V_1^0 + V_1^{90}); & M_{21} &= 0.5(V_2^0 + V_2^{90}); \\
 M_{12} &= 0.5(V_1^0 - V_1^{90}); & M_{22} &= 0.5(V_2^0 - V_2^{90}); \\
 M_{13} &= V_1^{45} - M_{11}; & M_{23} &= V_2^{45} - M_{21}; \\
 M_{14} &= V_1^{\otimes} - M_{11}; & M_{24} &= V_2^{\otimes} - M_{21}; \\
 \\ \\
 M_{31} &= 0.5(V_3^0 + V_3^{90}); & M_{41} &= 0.5(V_4^0 + V_4^{90}); \\
 M_{32} &= 0.5(V_3^0 - V_3^{90}); & M_{42} &= 0.5(V_4^0 - V_4^{90}); \\
 M_{33} &= V_3^{45} - M_{31}; & M_{43} &= V_4^{45} - M_{41}; \\
 M_{34} &= V_3^{\otimes} - M_{31}; & M_{44} &= V_4^{\otimes} - M_{41}.
 \end{aligned} \tag{6}$$

Here $V_{i=2;3;4}^{0;45;90;\otimes}$ - parameters of the Stokes vector of points of the digital image of the sample of the biological layer, measured for a series of linearly (0^0 ; 45^0 ; 90^0) and right-circular (\otimes) polarized laser beams

$$\begin{aligned}
V_{i=1}^{0;45;90;\otimes} &= I_0^{0;45;90;\otimes} + I_{90}^{0;45;90;\otimes}; \\
V_{i=2}^{0;45;90;\otimes} &= I_0^{0;45;90;\otimes} - I_{90}^{0;45;90;\otimes}; \\
V_{i=3}^{0;45;90;\otimes} &= I_{45}^{0;45;90;\otimes} - I_{135}^{0;45;90;\otimes}; \\
V_{i=4}^{0;45;90;\otimes} &= I_{\otimes}^{0;45;90;\otimes} + I_{\oplus}^{0;45;90;\otimes}.
\end{aligned} \tag{7}$$

Here $I_{0;45;90;135;\otimes;\oplus}$ - the intensity of light transmitted by an object passing through a linear polarizer θ with the angle of rotation of the transmission plane Θ : 0° ; 45° ; 90° ; 135° as well as through the system "quarter-wave plate - polarizer" of the polarization analysis unit object laser radiation.

Determination of the elements of the differential matrix of the 2nd order is carried out using the following relation¹⁷⁻²⁰

$$\begin{aligned}
\{\Delta m^2\} &= 0,5z^{-2} \times \\
&\times \begin{vmatrix} \ln 0.5(V_1^0 + V_1^{90}) & \ln \left(\frac{V_1^0 - V_1^{90}}{V_2^0 + V_2^{90}} \right) & \ln \left(\frac{V_1^{45} - 0.5(V_1^0 + V_1^{90})}{0.5(V_3^0 + V_3^{90})} \right) & \ln \left(\frac{V_1^{\otimes} - 0.5(V_1^0 + V_1^{90})}{0.5(V_4^0 + V_4^{90})} \right) \\ \ln \left(\frac{V_2^0 + V_2^{90}}{V_1^0 - V_1^{90}} \right) & \ln 0.5(V_2^0 - V_2^{90}) & \ln \left((V_2^{45} - 0.5(V_2^0 + V_2^{90})) \cdot 0.5(V_3^0 - V_3^{90}) \right) & \ln 0.5(V_4^0 - V_4^{90}) (V_2^{\otimes} - 0.5(V_2^0 + V_2^{90})) \\ \ln \left(\frac{0.5(V_3^0 + V_3^{90})}{V_1^{45} - 0.5(V_1^0 + V_1^{90})} \right) & \ln \left(0.5(V_3^0 - V_3^{90}) (V_2^{45} - 0.5(V_2^0 + V_2^{90})) \right) & \ln \left(V_3^{45} - 0.5(V_3^0 + V_3^{90}) \right) & \ln 0.5(V_3^{\otimes} - 0.5(V_3^0 + V_3^{90})) (V_4^0 - V_4^{90}) \\ \ln \left(\frac{0.5(V_4^0 + V_4^{90})}{V_1^{\otimes} - 0.5(V_1^0 + V_1^{90})} \right) & \ln 0.5(V_4^0 - V_4^{90}) (V_2^{\otimes} - 0.5(V_2^0 + V_2^{90})) & \ln 0.5(V_3^{\otimes} - 0.5(V_3^0 + V_3^{90})) (V_4^0 - V_4^{90}) & \ln \left(V_4^{\otimes} - 0.5(V_4^0 + V_4^{90}) \right) \end{vmatrix} \tag{8}
\end{aligned}$$

The matrix operator (8) serves as a basis for determining the set of MMI fluctuations of the parameters of linear and circular birefringence and dichroism.

3. Results and discussions

We investigated two groups of samples of histological sections of operably removed endometrial cysts of the 2nd (group 1) and 3rd degree (group 2) severity of endometriosis. The optical thickness of the layers of biological tissues varied within $2,11 \leq \tau \leq 2,39$, and the degree of depolarization $79\% \leq \Lambda \leq 88\%$. Under these conditions, the symmetry of the matrix operator $\{\Delta m^2\}$ acquires an almost diagonal form (relation (5)). Therefore, the statistical moments of the 1st – 4th orders, characterizing the distribution of the magnitude of the diagonal elements $\{\Delta m^2\}_{ii}$ of the second-order differential matrix, were considered as diagnostic parameters.

In fig.2 are shown histogram maps of the distribution of the magnitude of the diagonal element Δm_{22}^2 of histological sections of the endometrial biopsy with various pathologies.

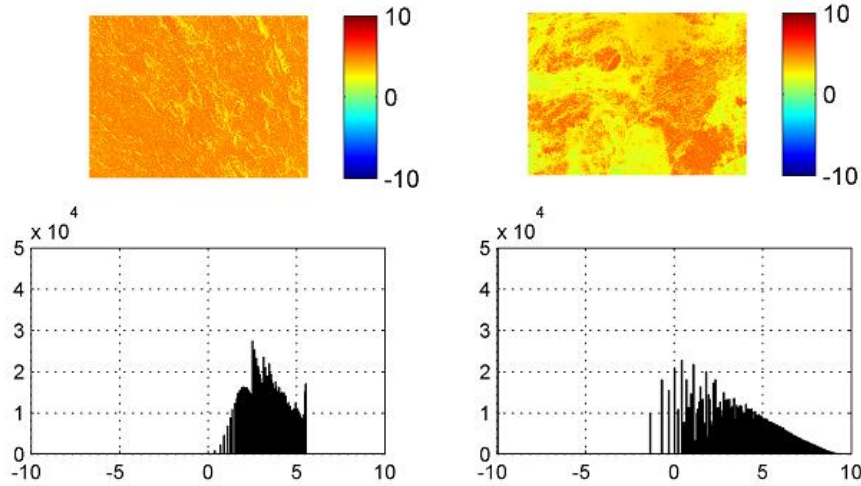


Fig. 2. Maps (fragments (1), (3)) and distribution histograms (fragments (2), (4)) of the magnitude of the diagonal element Δm_{22}^2 of the histological sections of the endometrial biopsy with various pathologies.

From the obtained data it is seen that endometriosis of the 3rd degree of severity is accompanied by a significant increase in the magnitude of linear birefringence. Quantitatively, this fact is illustrated by histograms of the distribution of the element $\Delta m_{22}^2 = \sigma_4^2(LB) - \sigma_1^2(LD) - \sigma_2^2(CD)$ of histological sections of the endometrial biopsy with varying severity of pathology, - fig. 1, fragments (2), (4). As can be seen, the range of the magnitude Δm_{22}^2 changes almost doubles. Physically, this can be associated with a trend $\sigma_4^2(LB) \uparrow$ due to the growth of linearly birefringent protein fibrils. Therefore, in the volume of such a multiple scattering pathological polycrystalline network, the dispersion of fluctuations of linear birefringence also increases.

Table 1 presents the average values and average errors of statistical ($Z_{i=1;2;3;4}$) parameters that characterize the distributions of the diagonal elements of the differential matrix of the 2nd order of endometrial samples for both groups of pathology.

For the possible clinical application of the method of differential Mueller-matrix mapping for each group of endometrial samples, the traditional for evidence-based medicine²¹⁻²³ operational characteristics were determined, which determine the diagnostic power of the method. Namely:

- sensitivity ($Se = \frac{a}{a+b} 100\%$);
- specificity ($Sp = \frac{c}{c+d} 100\%$);
- accuracy ($Ac = \frac{Se + Sp}{2}$),

where a and b the number of correct and incorrect diagnoses within group 2; c and d - also within group 1.

Table 1 Statistical moments of the 1st - 4th orders, which characterize the distributions of fluctuations of optical anisotropy of histological sections of endometrial biopsy of the 2nd (group 1) and 3rd degree (group 2) severity of endometriosis

Z_i	$\{\Delta m_{22}^2\}$		$\{\Delta m_{33}^2\}$		$\{\Delta m_{44}^2\}$	
	Group 1	Group 2	Group 1	Group 2	Group 1	Group 2
Z_1	2,61 ± 0,15	3,12 ± 0,17	2,81 ± 0,16	2,06 ± 0,11	3,18 ± 0,21	4,22 ± 0,31
Z_2	2,09 ± 0,12	4,16 ± 0,27	2,61 ± 0,14	3,11 ± 0,18	2,41 ± 0,16	3,74 ± 0,21
Z_3	0,92 ± 0,052	2,21 ± 0,13	1,19 ± 0,062	1,52 ± 0,082	0,61 ± 0,032	0,91 ± 0,062
Z_4	1,33 ± 0,071	3,72 ± 0,19	1,83 ± 0,11	1,27 ± 0,091	1,48 ± 0,077	2,97 ± 0,17

Conclusions

Comparative analysis of the set of statistical moments of the 1st - 4th orders revealed the following most sensitive to changes in the optical anisotropy of the layers of the endometrium against the background of a depolarized background of repeatedly scattered radiation (highlighted in gray):

- $\left\{ \Delta Z_2 \left(\{\Delta m_{22}^2\} \right) \leftrightarrow Ac = 87\% \right.$
- $\left. \Delta Z_3 \left(\{\Delta m_{22}^2\} \right) \leftrightarrow Ac = 91\% \right.$
- $\left. \Delta Z_4 \left(\{\Delta m_{22}^2\} \right) \leftrightarrow Ac = 93\% \right.$
- $\left\{ \Delta Z_3 \left(\{\Delta m_{33}^2\} \right) \leftrightarrow Ac = 79\% \right.$
- $\left. \Delta Z_4 \left(\{\Delta m_{44}^2\} \right) \leftrightarrow Ac = 90\% \right.$

The most sensitive and diagnostically accurate (excellent quality) were the statistical moments of the 3rd and 4th orders, which characterize the distributions of fluctuations in the parameters of linear birefringence.

References

- [1]. R. Ossikovski, V. Devlaminck, "General criterion for the physical realizability of the differential Mueller matrix," Opt. Lett. 39, 1216-1219 (2014).
- [2]. V. Devlaminck and R. Ossikovski, "Uniqueness of the differential Mueller matrix of uniform homogeneous media," Opt. Lett. 39, 3149-3152 (2014).
- [3]. V. Devlaminck, "Physical model of differential Mueller matrix for depolarizing uniform media," J. Opt. Soc. Am. 30, 2196-2204 (2013).
- [4]. Wang X. Propagation of polarized light in birefringent turbid media: a Monte Carlo study / X. Wang, L.-H. Wang // J. Biomed. Opt. – 2002. – Vol. 7. – P. 279-290.
- [5]. Tuchin V. V. Handbook of optical biomedical diagnostics / V. V. Tuchin. – Bellingham : SPIE Press, 2002. – 1110 p.
- [6]. Yao G. Two-dimensional depth-resolved Mueller matrix characterization of biological tissue by optical coherence tomography / G. Yao, L. V. Wang // Opt. Lett. – 1999. – V. 24. – P. 537-539.
- [7]. Tower T. T. Alignment Maps of Tissues: I. Microscopic Elliptical Polarimetry / T. T. Tower, R. T. Tranquillo // Biophys. J. – 2001. – Vol. 81. – P. 2954-2963.
- [8]. Lu S. Interpretation of Mueller matrices based on polar decomposition / S. Lu, R. A. Chipman // J. Opt. Soc. Am. A. – 1996. – Vol. 13. – P. 1106-1113.
- [9]. Ghosh Nirmalya. Techniques for fast and sensitive measurements of two-dimensional birefringence distributions / Nirmalya Ghosh, I. Alex Vitkin // Journal of Biomedical Optics. – 2011. – № 16(11). – P. 110801.
- [10]. V. V. Tuchin, L. Wang, and D. A. Zimnyakov, Optical Polarization in Biomedical Applications, New York, USA (2006).

- [11]. Ushenko, O. G., Grytsyuk, M., Ushenko, V. O., Bodnar, G. B., Vanchulyak, O., & Meglinskiy, I. (2018, January). Differential 3D Mueller-matrix mapping of optically anisotropic depolarizing biological layers. In *Thirteenth International Conference on Correlation Optics* (Vol. 10612, p. 106121I). International Society for Optics and Photonics.
- [12]. Ushenko, A.G., Dubolazov, O.V., Bachynsky, V.T., Peresunko, A.P., Vanchulyak, O.Y., "On the feasibilities of using the wavelet analysis of mueller matrix images of biological crystals," (2010) *Advances in Optical Technologies*, 162832.
- [13]. Zabolotna, N.L., Wojcik, W., Pavlov, S.V., Ushenko, O.G., Suleimenov, B., "Diagnostics of pathologically changed birefringent networks by means of phase Mueller matrix tomography," (2013) *Proceedings of SPIE - The International Society for Optical Engineering*, 8698, 86980.
- [14]. Ushenko, A.G., "Correlation Processing and Wavelet Analysis of Polarization Images of Biological Tissues," (2001) *Optics and Spectroscopy* (English translation of *Optika i Spektroskopiya*), 91 (5), pp. 773-778.
- [15]. Ushenko, A.G., Dubolazov, A.V., Ushenko, V.A., Novakovskaya, O.Y., "Statistical analysis of polarization-inhomogeneous Fourier spectra of laser radiation scattered by human skin in the tasks of differentiation of benign and malignant formations," (2016) *Journal of Biomedical Optics*, 21 (7), 071110.
- [16]. Bekshaev AY, Angelsky OV, Sviridova SV, Zenkova CY. Mechanical action of inhomogeneously polarized optical fields and detection of the internal energy flows. *Adv Opt Technol* 2011.
- [17]. Angelsky, O. V., Maksimyak, P. P., & Perun, T. O. (1993). Optical correlation method for measuring spatial complexity in optical fields. *Optics Letters*, 18(2), 90-92.
- [18]. Angelsky, O. V., Bekshaev, A. Y. A., Maksimyak, P. P., Maksimyak, A. P., & Hanson, S. G. (2018). Low-temperature laser-stimulated controllable generation of micro-bubbles in a water suspension of absorptive colloid particles. *Optics Express*, 26(11), 13995-14009.
- [19]. Angelsky, O. V. (2007). Optical correlation techniques and applications. *Optical correlation techniques and applications* (pp. 1-270).
- [20]. Angelsky, O. V., Ushenko, A. G., Pishak, V. P., Burkovets, D. N., Yermolenko, S. B., Pishak, O. V., & Ushenko, Y. A. (2000). Coherent introscopy of phase-inhomogeneous surfaces and layers. Paper presented at the *Proceedings of SPIE - the International Society for Optical Engineering*, 4016 413-418.
- [21]. "Cassidy, "Basic concepts of statistical analysis for surgical research," *Journal of Surgical Research* 128,199-206 (2005).
- [22]. C. S. Davis, *Statistical methods of the analysis of repeated measurements*, 744, New York: Springer-Verlag (2002).
- [23]. A. Petrie, B. Sabin, *Medical Statistics at a Glance*, pp. 157, Blackwell Publishing (2005).